JOURNAL OF GEOPHYSICAL RESEARCH, VOL. 89, NO. A7, PAGES 5386–5394, JULY 1, 1984

Distribution of Solar Wind Angular Momentum Between Particles and Magnetic Field: Inferences About the Alfvén Critical Point From Helios Observations

E. MARSCH AND A. K. RICHTER

Max-Planck-Institut für Aeronomie

We first discuss theoretically the relative importance and the behavior of the two basic terms adding to the total angular momentum flux, the angular momentum of the particles (electrons, protons and alpha particles) and of the magnetic field stresses, respectively. Second, we analyze these two quantities with respect to their dependence on heliocentric distance by using the Helios 1 and 2 plasma and interplanetary magnetic field observations between 0.3 and 1 AU classified according to low-speed (<400 km s^{-1}), intermediate (400–600 km s^{-1}), and high-speed (>600 km s^{-1}) solar wind for the 1975–1976 epoch. Applying now these results as well as various combinations of the constants of motion for the solar wind (such as the total angular momentum flux, the mass flux, and the magnetic flux) and their observational constraints, as deduced earlier by Marsch and Richter (1984), we finally present various methods (1) to derive the values of several characteristic solar wind plasma and magnetic field parameters at the Alfvén critical points, (2) to estimate their locations above the solar surface, and (3) to obtain the radial slope of the associated solar wind velocity profiles for the three solar wind classes separately.

1. INTRODUCTION

The angular momentum that is lost by the sun to the expanding corona and the solar wind is one of the sun's key features from an astrophysical point of view. *Weber and Davis* [1967] (WD), in a pioneering paper, were the first to succeed in self-consistently solving the fluid equations, which describe the transport of particles' mechanical and magnetic field stresses in the expanding solar wind. The angular momentum per atomic mass unit L lost by the sun is simply given by the formula $L = \Omega r_A^2$ corresponding to rigid body corotation out to the so-called Alfvén radius r_A (here Ω denotes the sun's angular rotation frequency resulting in a corotational speed of $\Omega R_S = 2$ km s^{-1} at the solar surface on the sun's equator). There have been many early attempts to estimate L by in situ observations at 1 AU [see *Lazarus and Goldstein*, 1971, and references therein]. All these efforts resulted in estimates of the azimuthal flow velocity u_ϕ at 1 AU ranging from about 1 to 10 km s^{-1}, values that were often larger than predicted by the WD model. Also, *Lazarus and Goldstein* [1971] found that the dominant contribution to L arises from the particles' mechanical stresses L_P and not from the magnetic field stresses L_M, an observation considered as being at variance with the theoretical predictions of the WD model.

From a recent determination of L by Helios measurements, *Pizzo et al.* [1983] yielded values somewhat smaller than previous ones. They found the total angular momentum flux per steradian to be about 0.2–0.3 10^{30} dyn cm sr^{-1} and a distribution of fluxes between particles and fields very near the 1:3 ratio of the WD model. Another important new finding in their study was that the alpha particle flow direction differed considerably from that of the protons in high-speed streams. This differential movement aligned with the local magnetic field (that on the average coincides with the Parker spiral) leads to a negative contribution of the alphas to L. It is of the order of -0.1 10^{30} dyn cm sr^{-1} which offsets the protons' angular momentum. *Pizzo et al.* [1983] found that the observed total angular momentum depends on the flow speed with a clear indication for slow wind to carry positive (in the sense of corotation) and fast wind to exhibit even negative angular momentum. This was interpreted to be due to interplanetary stream interactions. The data set used was biased toward intermediate and high-speed solar wind (>400 km s^{-1}), whereas the Mariner 5 data used by *Lazarus and Goldstein* [1971] were mainly sampled over slow solar wind with velocities of ~ 400 km s^{-1}.

However, in all these comparisons it has been overlooked entirely that the theoretical result for $L_P/L_M \approx 1/3$ of *Weber and Davis* [1967] pertained to very specific boundary conditions at the earth ($u_{R_E} = 400$ km s^{-1}) and to a polytropic outflow. Their calculation was only meant to be an illustrative example and by no means to hold generally. Unfortunately, the ratio $L_P/L_M = 1/3$ was later on referred to as a canonical number, and experimenters apparently forgot about the very restricted validity of the original model calculations by WD. However, their theoretical framework was indeed more general than indicated by the illustrative model calculation. *Meyer and Pfirsch* [1969], *Weber and Davis* [1970], and *Acuna and Whang* [1976] have generalized the model to the case of a multicomponent, anisotropic plasma. These extensions of the original model have been necessitated as well by the recent Helios plasma observations, particular in perihelion at 0.3 AU, that suggest to treat the alpha particles not any longer as minor ions but as major constituents of the solar wind plasma (see also review by *Neugebauer* [1981]).

Within this general theoretical framework, we show in this paper that one may conceive a wide variety of solar wind flows ranging from an expansion where most of the angular momentum is carried by the particles to a solar wind where L is dominated by magnetic field stresses. The ratio of L_P/L_M is found to be entirely determined by the Mach number profile, i.e., by the radial profiles of the Alfvén speed and the radial bulk velocity component u_r. Our presentation supplements the theoretical papers by *Weber and Davis* [1967] and *Acuna and*

Paper number 4A0444.
0148-0227/84/004A-0444$05.00

Whang [1976] and intends to clarify the important issue on how the total angular momentum is distributed between particles and fields. Concerning the Helios observations to be discussed below we aime to complement the work by *Pizzo et al.* [1983] who presented the most recent and reliable determination of the solar wind angular momentum flux from Helios data. As a result, they also derived an estimate of the Alfvén radius ranging between 12 and 14 R_S. We will use a subset of their data and shall not again extensively discuss the experimental problems. A second and major goal of our paper is to derive additional, critical parameters at the Alfvén point r_A. These are, the flow speed itself, that is equal to the Alfvén speed by definition, the critical particle number density, the magnetic field strength, and the radial acceleration of the flow.

The paper is organized as follows. The first section contains the theoretical discussion on the specific angular momenta L_P and L_M that constitute the total L. Various limits, as a function of heliocentric distance, for the ratio L_P/L_M are evaluated. The second section presents Helios observations between 0.3 and 1 AU, which can serve to infer the plasma and magnetic field parameters at the Alfvén critical point. A final section presents a summary and conclusions.

2. Angular Momentum and its Distribution Between Particles and Field

This section is devoted to a thorough discussion of the total solar wind angular momentum and its distribution between the magnetic field and the primary particle constituents of the plasma which are electrons, protons and alpha particles in order of numerical abundance. One of the key features of the WD model and its generalization to a multicomponent, anisotropic plasma is the prediction of the sun's angular momentum loss rate $\dot{M}L$, where

$$\dot{M} = \rho u_r r^2 \tag{1}$$

is the total mass lost to the expanding solar wind per second and steradian (typically of the order of 10^{11} g s^{-1}/sr) and, after *Meyer and Pfirsch* [1969], L is the specific angular momentum per AMU given by

$$L = r\left[u_\phi - \frac{B_r B_\phi}{4\pi\rho u_r}\left(1 - \frac{4\pi}{B^2}(p_\parallel - p_\perp)\right)\right] \tag{2}$$

The total plasma mass density is denoted by ρ, the bulk flow velocity of the wind by $\mathbf{u} = u_r\mathbf{e}_r + u_\phi\mathbf{e}_\phi$, and the magnetic field by $\mathbf{B} = B_r\mathbf{e}_r + B_\phi\mathbf{e}_\phi$. The mass density is essentially given by $\rho = n_\alpha m_\alpha + n_p m_p$, whereby the alpha abundance n_α/n_p is typically a few percent with an average of 5% in high-velocity streams [see *Feldman et al.*, 1977; *Schwenn*, 1983]. The WD model describes the solar wind evolution under time stationary conditions in the ecliptic plane with the heliocentric distance r being the only independent variable. In (2) the correction factor for the magnetic stresses arises from the total thermal pressure anisotropy. For the multicomponent plasma, *Marsch and Richter* [1984] found a ratio $A = p_\perp/p_\parallel$ of about 0.9. However, the anisotropies of the individual species may be more pronounced. Thus the correction factor in (2) is almost equal to 1 for the data analyzed here.

The specific angular momentum L is a constant of motion for the expanding solar wind. The condition of continuity of u_ϕ and B_ϕ through the Alfvén critical point, where the Alfvén Mach number is $M_A = 1$, $M_A = u_r/v_{Ar}$, $v_{Ar} = B_r(4\pi\rho)^{-1/2}$ $(1 - 4\pi/B^2(p_\parallel - p_\perp))^{1/2}$, requires according to *Weber and Davis* [1967] and *Meyer and Pfirsch* [1969] that

$$L = \Omega r_A^2 \tag{3}$$

This equation allows to determine r_A from in situ measurements of L, since according to (2), L is derivable from plasma and magnetic field data and the solar rotation frequency Ω is known.

There is another key feature of the WD model associated wtih L. The model predicts the distribution of the total angular momentum $L = L_P + L_M$ between the particles L_P and the field L_M. However, the ratio L_P/L_M generally is not a constant of motion but changes with radial distance from the sun as the components of $\mathbf{u}$ and $\mathbf{B}$, and as the mass density ρ evolve radially. It is worth emphasizing this point, since there seems to be some confusion in the literature on this point. The figure $L_P/L_M = 1/3$, given by WD, is not a general feature of how the sun distributes its angular momentum loss between the particles' mechanical and field stresses. This ratio simply reflects the boundary values at r_A and at $R_E = 1$ AU as chosen by Weber and Davis to model a slow solar wind with a flow speed of $u_{R_E} = 400$ km s^{-1}.

In order to clarify this important issue, some algebraic calculations are required that have not been provided by WD, but which follow straightforwardly. Here and in the remainder of this paper, we restrict ourselves to the case $A = 1$, which is suggested by the almost isotropic total pressure found by *Marsch and Richter* [1984].

From the equations of *Weber and Davis* [1967] and the definition of (2) we then find the following expressions:

$$L_P = \Omega r^2\left(1 - \left(\frac{r_A}{r}\right)^2 M_A^2\right)\Big/(1 - M_A^2) \tag{4a}$$

$$L_M = -\Omega r^2\left(1 - \left(\frac{r_A}{r}\right)^2\right)\Big/(1 - M_A^2) \tag{4b}$$

It is readily shown that $L_P + L_M = L = \Omega r_A^2$. We may also express the specific angular momenta in directly measurable quantities as

$$L_P = r u_\phi \tag{5a}$$

$$L_M = -r\frac{B_\phi}{4\pi}\frac{F_B}{\dot{M}} \tag{5b}$$

where Gauss' law yields the constant F_B to be

$$F_B = r^2 B_r \tag{6}$$

Exploiting the equation of continuity (1) and (6), we obtain the result

$$M_A^2\left(\frac{r_A}{r}\right)^2 = \frac{u_r}{u_{r_A}} \tag{7}$$

where u_{r_A} is the flow speed at the Alfvén point. Furthermore, we define the logarithmic derivative of u_r with respect to r at r_A as

$$u' = \left.\frac{d\ln u_r}{d\ln r^2}\right|_{r_A} \tag{8}$$

There are some important limits for $L_{P,M}$ that can be obtained at the solar surface and at infinity. For any solution of the radial flow profile with $u_r \to 0$ for $r \to 0$, we find that

$$L_P|_{r\to 0} \approx \Omega r^2 \approx 0 \tag{9a}$$

$$L_M|_{r\to 0} \approx \Omega r_A^2 \tag{9b}$$

Therefore, close to the sun where $r \ll r_A$ the angular momentum resides in the magnetic field, whereas the particles' mechanical angular momentum due to corotation is much smaller. The principal effect of the spiral field is to enforce near-corotation of the plasma below the Alfvén point, however, with little radial acceleration of the wind [*Barnes*, 1974].

At the Alfvén critical point, an expansion of M_A^2 about 1 yields

$$L_P|_{r_A} = \Omega r_A^2 \frac{u'}{1+u'} \tag{10a}$$

$$L_M|_{r_A} = \Omega r_A^2 \frac{1}{1+u'} \tag{10b}$$

or $L_P/L_M = u'$ at $r = r_A$. Since we are interested in coronal expansion and in a radially accelerating outflow of the plasma, we only consider the range $0 < u' < \infty$ corresponding to $du_r/dr > 0$. Besides, the unphysical solution $u' = -1$ yields infinite energy and is associated with an expansion at constant density and has thus to be discarded. Equations (10*a*), (10*b*) indicate that the relative importance of particles' and field stresses in L is determined by the slope of the radial flow profile at the critical point. Smooth gradients ($u' < 1$) are associated with dominating field stresses. The case $u' = 1$ corresponds to an equipartition where half of the total $L = \Omega r_A^2$ resides in particles and fields, respectively. Finally, steep, logarithmic, radial gradients of the velocity at r_A point to a situation where the solar wind angular momentum is mostly carried by the particles. However, these statements only refer to the Alfvén point. Asymptotically at large heliocentric distances, the situation may be even reversed. Here we find, according to *Weber and Davis* [1967] with $M_A^2 \gg 1$, and $r \gg r_A$, the result

$$L_P|_{r\to\infty} = \Omega r_A^2(1 - u_{r_A}/u_r) \tag{11a}$$

$$L_M|_{r\to\infty} = \Omega r_A^2 u_{r_A}/u_r \tag{11b}$$

Apparently, the ratio of the asymptotic flow speed to the Alfvén speed at the critical point determines the values of L_P and L_M. We may summarize our discussion for the distribution of the total angular momentum between particles and field as follows: Close to the solar surface ($r \ll r_A$) the magnetic field stresses dominate L, and in case of a solar wind that starts with zero radial velocity, we obtain

$$L_P/L_M|_{r\to 0} = 0 \tag{12a}$$

At the Alfvén point we find

$$L_P/L_M|_{r_A} = u' \tag{12b}$$

whereas at infinity ($r \gg r_A$) the result is

$$L_P/L_M|_{r\to\infty} = u_r/u_{r_A} - 1 \tag{12c}$$

Clearly, unlike $L = L_P + L_M$ that is strictly conserved, the ratio L_P/L_M varies considerably in dependence upon the detailed radial flow velocity profile. Whether an in situ observer far from the Alfvén point concludes that the angular momentum loss is mainly due to magnetic stresses depends on the observed flow speed u_r and the critical speed u_{r_A}, which at present can only indirectly be inferred. If $u_\infty/u_{r_A} < 2$ the solar wind angular momentum at large heliocentric distances is mostly owing to magnetic stresses. However, if the wind passes slowly through the Alfvén point but then progressively accelerates to values of $u_\infty > 2u_{r_A}$, we would find the angular momentum to be carried predominantly by the particles. Our discussion suggests that the real solar wind, being highly structured in, e.g., recurrent fast streams and slow dense plasma, should exhibit a variety of different situations.

We have shown that in situ observations of u_ϕ and B_ϕ, and of the constants of motion $\dot{M}$ and F_B provide a unique opportunity to directly determine L_P and L_M and thus the key plasma parameters at the Alfvénic point. First, as mentioned before, the Alfvén radius results from $r_A = (L/\Omega)^{1/2}$. Secondly, L_P/L_M at $r \gg r_A$ directly gives u_{r_A} via the formula

$$u_{r_A} = u_r(1 + L_P/L_M)^{-1} \tag{13}$$

The density at the Alfvén point is precisely fixed by the constants of motion

$$\rho_A = 4\pi(\dot{M}/F_B)^2 \tag{14}$$

as readily follows from (1) and (6). Thus by exploiting the continuity equation, u_{r_A} may be determined from (1) and (3) or, vice versa, after having evaluated u_{r_A} from (13), we may subsequently calculate r_A from (1). Notice that (14) provides a rather accurate estimate of ρ_A, even if the flux tubes expand differently than r^{-2}. Clearly, the radial component of the magnetic field B_{r_A} follows also directly from (3) and (6). In contrast, u_ϕ and B_ϕ are entirely determined by u' at r_A and can therefore not be estimated by our "remote sensing" technique of the Alfvén critical point.

3. Helios Observations and Inferred Parameters at the Alfvén Point

The data set used for the present study has been extensively described by *Rosenbauer et al.* [1977], *Marsch et al.* [1982*a*, *b*], *Pilipp et al.* [1981], and *Neubauer et al.* [1977*a*, *b*]. The solar wind observed by the Helios probes during the near-minimum epoch of solar activity of the past cycle was characterized by two large recurrent high-speed streams associated with a dipole sector structure [*Behannon et al.*, 1981]. Although the Helios 2 observations are about 1 year later than those of Helios 1, both probes essentially viewed the same kind of solar wind. Our investigation uses the three-dimensional ion plasma data that provide the full flow velocity vectors of protons and alphas. As mentioned before, the azimuthal component of the bulk velocity u_ϕ is extremely difficult to measure. *Pizzo et al.* [1983] have given a very thorough discussion on this problem. Thus we refer the reader to their paper for further details. Since we use the same data set as they did, all their estimates of measurement uncertainties and probable errors also apply to our analysis.

In Figure 1 we have plotted the specific angular momentum of the particles' (mechanical angular momentum per AMU) L_P and of the magnetic field L_M as defined in equations (5*a*), (5*b*). Numerical values of the conserved quantities F_B and $\dot{M}$, frequently used from now on, are given in Table 1, which also contains solar wind parameters averaged over heliocentric distance between 0.3 and 1 AU. Note, that the scales for L_P (top panel) and L_M (bottom panel) are different. Both parameters are given in astronomical units times kilometer s^{-1} and are displayed versus heliocentric distance in astronomical units. The thick error bars represent the standard deviation of the means, shown, respectively, at the right-hand edge of the frame. We find the total mean values for our data set as $L_P = (0.8 \pm 18.4)$ (AU km s^{-1}) and $L_M = (1.1 \pm 2.3)$ (AU km s^{-1}). It should be noted, in order to avoid confusion, that here

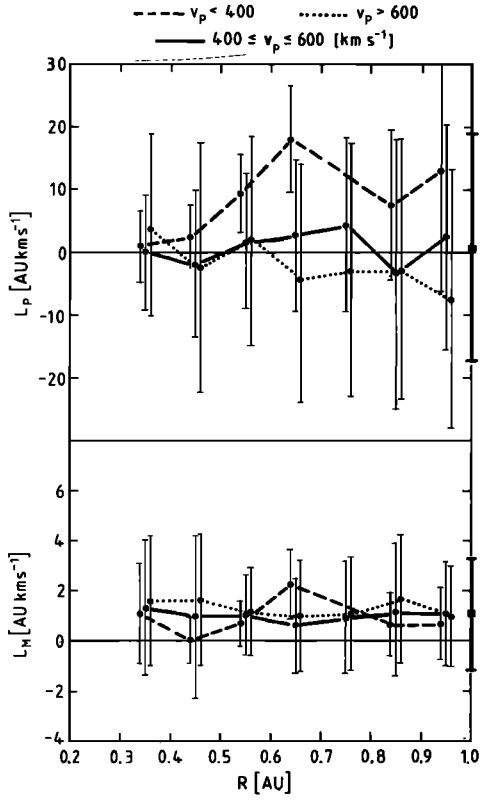

Fig. 1. Specific angular momentum of the particles L_P in (AU km s^{-1}) plotted versus heliocentric distance (top) and of the magnetic field L_M in the bottom panel. Data correspond to low (dashed), intermediate (continuous), and high-speed solar wind (dotted line). Standard deviation bars are slightly displaced in order to avoid overlapping. Averages have been performed over radial distance bins of 0.1 AU in width.

and in Table 1 we quote errors in terms of standard deviations referring to typical fluctuations in the data. The error of the mean is much smaller by a factor of 94 for the entire data set with $N = 8873$ spectra. However, we feel such an error estimate is less informative and probably somewhat overoptimistic in view of our data sampling technique and the temporal and spatial variability of the solar wind.

All the points in Figure 1 represent averages over radial distance bins (0.1 AU in width) and are plotted with their typical rms deviations, whereby the bars have been slightly displaced to avoid overlapping. The dashed lines correspond to low-speed wind ($v_p < 400$ km s^{-1}), the continuous lines to intermediate flow speeds ($400 \leq v_p \leq 600$ km s^{-1}), and the dotted curves pertain to high speed solar wind streams ($v_p > 600$ km s^{-1}). The low- and high-speed classes mostly contain data which are not associated with stream interfaces. In contrast, in the bin pertinent to intermediate speeds data have been sampled which correspond to the leading edges of recurrent streams and to interaction regions. These data have been lumped together with data from noncompressed plasma of the trailing edges of fast streams.

Inspection of the top panel shows that there is considerable scatter in the data which tends to increase at larger heliocentric distances. This trend is already obvious in the raw data and has been interpreted by *Pizzo et al.* [1983] as being caused by stream interaction dynamics. Apparently, L_P tends to increase with radius in low and to decrease and become negative in high-speed solar wind. The mainly negative values of L_P in fast streams are essentially due to the alpha particles, which travel faster than the protons at a speed which is a considerable fraction of the Alfvén speed [*Asbridge et al.*, 1976; *Marsch et al.*, 1982*b*] and much larger than $|u_\phi|$. Since their differential streaming is aligned with the Parker spiral, they tend to exhibit a negative $u_{\phi\alpha}$. The mean values of L_P averaged over radial distance but yet binned according to flow speed are given in Table 1.

Inspection of Figure 1 shows that in the intermediate speed regime L_P fluctuates about zero with no apparent radial trend. From an eyeball fit one may get the impression that the variations in L_P in dependence on flow speed become less pronounced in perihelion. This might suggest that the spread in the data at larger heliocentric distances are actually of interplanetary origin and not an indication of a primordial bulk speed dependence of L_P already in the corona. Certainly, negative L_P cannot originate in the corona, if the plasma initially is partly corrotating with the sun. This objection casts doubt on whether L_P can be used at all to infer plasma parameters about the Alfvén point. Despite these notes of caution we will later on take our observations at face value and assume that the presented theoretical formulae can still be applied to analyze our data.

If we direct our attention now to the lower part of Figure 1 it becomes readily apparent that L_M is by far more constant than L_P and does only weakly depend on radius as well as on solar wind flow speed. The total average of $L_M = (1.07 \pm 2.25)$ (AU km s^{-1}) would correspond to an equivalent mechanical azimuthal velocity of 1 km/s at 1 AU. This independence of L_M on the actual stream structure of the solar wind is truely remarkable. Similar results have been found by *Pizzo et al.* [1983, see their Table 2]. They quoted a mean of $\dot{M}L_M = 0.19$ ($\times 10^{30}$ dyn cm/sr) for almost the entire Helios mission that compares well with our mean of $\dot{M}L_M = 0.16 \pm 2.64$ ($\times 10^{30}$ dyn cm/sr). In contrast to L_P, the quoted mean of L_M is a rather accurately determined figure, since the quantity $\dot{M}L_M$ is relatively insensitive to errors in the components of the magnetic field which is not so radially oriented as the plasma flow.

TABLE 1. Solar Wind Parameters Averaged Over Heliocentric Distance Between 0.3 and 1 AU

Parameter	$v_p < 400$ km s^{-1}	$400 \leq v_p \leq 600$ km s^{-1}	600 km s^{-1} $< v_p$	Total
u_r, km s^{-1}	357 ± 28	503 ± 66	676 ± 47	560 ± 125
u_ϕ, km s^{-1}	11.82 ± 18.13	1.80 ± 21.16	-2.02 ± 34.82	1.45 ± 28.11
B_r, nT	5.97 ± 6.89	7.63 ± 7.61	10.91 ± 11.25	8.86 ± 9.52
B_ϕ, nT	-2.72 ± 6.39	-1.96 ± 5.64	-2.95 ± 8.18	-2.50 ± 6.98
F_B, nT AU^2/sr	2.86 ± 1.87	3.54 ± 1.73	3.15 ± 1.49	3.28 ± 1.67
$\dot{M}$, 10^{11} gs^{-1}/sr	1.49 ± 0.61	1.09 ± 0.62	0.81 ± 0.22	1.02 ± 0.53
L_M, AU km s^{-1}	0.82 ± 1.51	1.06 ± 2.29	1.16 ± 2.39	1.07 ± 2.25
L_P, AU km s^{-1}	9.88 ± 15.47	1.48 ± 16.66	-2.59 ± 19.71	0.80 ± 18.38
L, AU km s^{-1}	10.6 ± 16	2.34 ± 17	-1.55 ± 21	1.71 ± 19
L_M, AU km s^{-1}	1.18 ± 0.82	1.76 ± 0.57	1.40 ± 0.20	1.45 ± 0.28

From a theoretical point of view the relative constancy of L_M should imply that also L_P should be constant, since their sum equals L, which is a strict constant of motion. Therefore the variability in L_P might actually be a spurious effect due to the real stream structure of the solar wind which has not been considered in the homogeneous WD model. If, namely, the solar wind has already attained its asymptotic flow speed u_∞ at distances below the Helios perihelion, then L_P should, as well as L_M, be strictly constant according to (11*a*), (11*b*). By using (11*b*), (1), and (14), we can derive a simple expression for L_M in terms of constants of motion and of the asymptotic flow speed u_∞ as

$$L_M = \frac{\Omega F_B^2}{4\pi \dot{M} u_\infty} \tag{15}$$

This relation also follows by directly inserting the Parker spiral relation $B_\phi = -\Omega r B_r/u_\infty$ as applying to the asymptotic flow regime into equation (5*b*). Note that the expression (15) only involves constants of motion associated with the radial velocity and magnetic field components. Numerical parameters for three solar wind speed classes are contained in the last row of Table 1. As can be seen, the figures for L_M estimated directly from B_ϕ in (5*b*) agree remarkably well with those derived from (15). This is an impessing verification of the correctness of the WD model in describing the sun's angular momentum loss associated with magnetic stresses. Note also that the alpha particles which have been neglected so far in other studies are an important constituent of the plasma with respect to its bulk motion. This has been emphasized and demonstrated before by *Pizzo et al.* [1983]. If we can assume that L_P is always positive and that negative values beyond 0.3 AU arise from interplanetary dynamics, then we can put a very rigorous lower limit on the Alfvén critical radius by the inequality $L_M \leq L = \Omega r_A^2$. This yields the relation

$$r_A/R_S \geq (L_M/\Omega R_S^2)^{1/2} \tag{16}$$

Since L_M is not sensitive to flow speed, we may take the directly measured total average giving $r_A \geq 11\ R_S$. Unless we allow for negative L_P, this value for r_A ought to be considered as a lower limit for the Alfvén critical radius of the solar wind! Additional angular momentum carried away by the particles in the sense of corotation with the sun can only enhance the above estimate.

Let us now present additional inferences about critical parameters. Above we have shown that the fluid parameters at the Alfvénic point can be expressed by the constants of motion. By using the results in Table 1, we can determine the critical parameters as summarized in the top rows of Table 2. Note that L turned out to be negative on the average for high-velocity wind. Therefore, we could not estimate the corresponding value of r_A. The numbers in the top part of Table 2 relate to the respective Alfvén radius in each column, whereas the other figures in brackets are based upon our total average value of $r_A = 13.6\ R_S$. It is worth emphasizing that the critical density does not explicitly depend on the somewhat inaccurate values for r_A (or L) and thus is rather well determined. All the other numerical estimates crucially depend on the accuracy of L. Note the very high velocity inferred at the Alfvénic point in high-speed streams. In contrast, for the slow solar wind we find the Alfvénic point to be associated with a much lower flow speed. Nevertheless, in view of their possible errors and dependence on model assumptions detailed in section 2, the results in Table 2 should not be taken at face value but rather as semi-quantitative.

The bottom part of Table 2 presents critical parameters as primarily inferred from equation (13), which allows to directly determine u_{r_A} from the measured ratio L_P/L_M and the flow speed u_r. The corresponding Alfvén critical radius r_A then readily follows from the equation of continuity (1), and, subsequently, B_{r_A} flows from equation (6). Figures given in brackets correspond to our total data set irrespective of the sign of L_P, whereas the other numbers relate to the subset of data with a positive L_P as expected for partly corotating particles. The data are shown in Figure 2 binned according to radial distance and flow speed (open little boxes for $v_p > 600$ km s^{-1}, open triangles for $400 \leq v_p \leq 600$ km s^{-1}, and open circles for low-speed wind with $v_p < 400$ km s^{-1}). Solid symbols at the limb of the frame indicate the bracketed averages from the bottom part of Table 2. The asterisks on the left-hand side represent the values inferred from the parameters obtained by averaging over the entire data set.

It should be noted that the result determined from r_A and u_{r_A}, on the other hand, are not really independent from a strict mathematical point of view. They depend similarly on the most uncertain parameter L_P/L_M. By exploiting (1) and (13)–(15), we have

$$r_A^2 = \dot{M}/(\rho_A u_{r_A}) = F_B^2/(4\pi \dot{M} u_r) \cdot (1 + L_P/L_M)$$
$$= L_M/\Omega(1 + L_P/L_M)$$

which is equal to equation (3), although, from the point of view of the data in Tables 1 and 2 representing averages over many individual spectra pertaining to various velocity or radial distance bins, the two methods employed are not strictly equal. Still, both of them yield a set of compatible and equivalent critical parameters, even though obtained via different sampling procedures. The results of the first method are due to averages of $L = L_M + L_P$, whereby also negative L_P were included. However, the nonbracketed numbers in Table

TABLE 2. Solar Wind Parameters at the Alfvén Critical Point

Parameter	$v_p < 400$ km s^{-1}	$400 \leq v_p \leq 600$ km s^{-1}	600 km s$^{-1} < v_p$	Total	Derived From
n_A, cm^{-3}	4017	1403	978	1431	F_B, $\dot{M}$
r_A, R_S	33.8	15.9	(13.6)	13.6	L
u_{r_A}, km s^{-1}	(248) 40	(519) 380	(553)	476	$\dot{M}$, n_A, r_A
B_{r_A}, nT	(721) 116	(892) 647	(787)	819	F_B, r_A
r_A, R_S	(40.8) 48.9	(21.4) 30.9	17.3	16.6	$\dot{M}$, n_A, u_{r_A}
u_{r_A}, km s^{-1}	(28) 52	(209) 205	233	320	u_r, L_P/L_M
B_{r_A}, nT	(81) 151	(359) 351	334	554	F_B, r_A
L_P/L_M	(12.1) 9.8	(1.4) 2.6	(−2.2) 1.9	0.8	L_P/L_M
$(du_r/dr)\|r = r_A$, km s^{-1}/R_S	21	35	51	31	u_{r_A}, r_A L_P/L_M
Number of spectra	1186	3759	3928	8873	

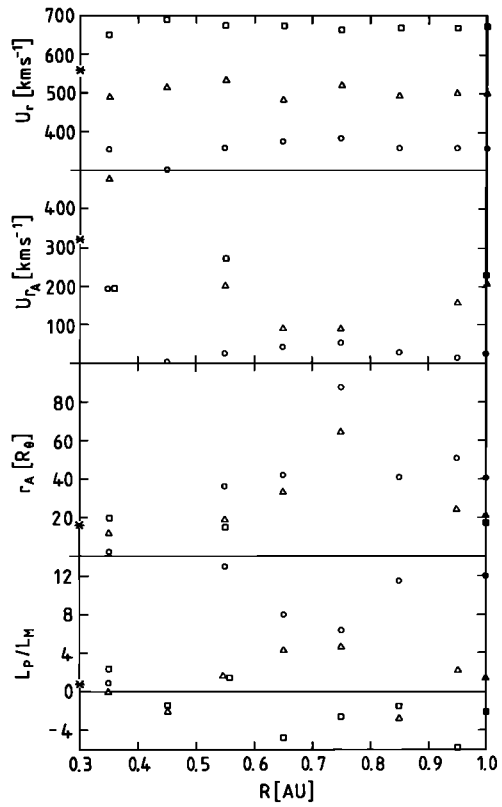

Fig. 2. The average radial bulk velocity component u_r as observed in situ (little boxes for $v_p > 600$ km s^{-1}, triangles for $400 \leq v_p \leq 600$ km s^{-1}, and circles for $v_p < 400$ km s^{-1}), the inferred flow speed at the Alfvén critical point, the corresponding radius in solar radii, and finally the in situ measured ratio L_P/L_M are shown versus radial distance from the sun in astronomical units. Note the different scales. Asterisks indicate averages over the whole data set without binning. Full solid symbols at the right-hand side refer to averages obtained by binning the entire data according to speed.

2, derived by the second method exploiting equation (13), are based only on the positive values for L_P given in Figure 2.

Since L_P/L_M is the primary information in Figure 2, all the scatter in the L_P/L_M data is reflected in large variances of r_A and u_{r_A}. As L_M was found to be almost independent of radial distance (compare with Figure 1), radial trends in the bottom panel of Figure 2 for L_P/L_M mirror the radial dependence of L_P shown in the top of Figure 1. Apparently, values of about 10 can be found for L_P/L_M in low-speed wind, whereas in fast streams negative values of about -2 are frequently observed. The two positive values at 0.35 and 0.55 AU are used to infer the number given in column three (lower part) of Table 2. This selection procedure is admittedly somewhat arbitrary, and the derived conclusions are essentially qualitative in nature. Thus we consider our numbers in Table 2, column 3, as semiquantitative and not very rigorous estimates.

Note that the total average for L_P/L_M is 0.8. This figure is slightly smaller than 1 due to the fact that the negative values in high-speed flow cancel the large positive values in slow solar wind. Note that our data set is somewhat biased toward high-velocity streams as can be seen from the last panel of Table 2 giving the respective number of spectra used. According to (13) the subset of low-speed solar wind data yields a critical Alfvén radius of about 40 R_S and, correspondingly, a critical Alfvén speed of only $u_{r_A} = 40$–50 km s^{-1}, which is somewhat more than a tenth of the asymptotic flow speed of 357 km s^{-1} (see Table 1). The two estimates of r_A and u_{r_A} based upon L and L_P/L_M are in fair agreement considering the many experimental limitations of the method employed.

For sake of completeness, we have also shown all the data sampled in solar wind flow of intermediate speed corresponding to stream-stream interaction regions and trailing edges of fast streams during the time period under consideration. Apparently, this subset of data most severely violates the model assumption of a homogeneous flow. Thus the inferred parametes should be considered with caution. However, the parameters pertaining to the body of fast recurrent high-speed streams should be more reliable, at least in perihelion. The two points with a positive L_P/L_M (average value 1.9) yield an Alfvén radius of about 17 R_S in fair accord with the one (13.6 R_S) inferred directly from L. As mentioned already, our data set is biased toward high-speed solar wind. By this reason our total averages are certainly more representative for high- than for low-speed solar wind.

From the last two columns of Table 1 and Table 2 it becomes apparent that in the average solar wind we find a near equipartition between particles' mechanical and magnetic field stresses. Whether the trend toward negative L_P in fast wind is real or due to interplanetary dynamical processes, or even spurious (since we also found positive values in periherlion) remains an open question, that could only be decided by in situ plasma measurements below 0.3 AU. Negative values of L_P in the corona appear to be unlikely from a theoretical point of view, because they would indicate anticorotating flow of the plasma, which does not seem to be plausible. We finally briefly mention the critical, radial magnetic field component (B_{r_A}) inferred from our remote plasma measurements. The values quoted in the top part of Table 2 result directly from Gauss' law for given r_A, whereas B_{r_A} quoted in the bottom part was determined by exploiting the definition of the radial Alfvén speed being equal to the estimated u_{r_A} at the critical point. Generally, the B_{r_A} values based upon r_A estimated first are somewhat larger than those that are determined from $B_{r_A} = u_{r_A}(4\pi\rho_A)^{1/2}$, where u_{r_A} was estimated first. However, all the trends are consistent, and for low-speed wind there is even fair agreement between the figures as calculated by these two different methods.

Finally, we shall concentrate on the radial acceleration of the solar wind flow at the Alfvénic point. Equations (10*a*), (10*b*) offer an interesting possibility to estimate du_r/dr at $r = r_A$. Let us assume that the asymptotic value for L_P/L_M is already reached at r_A and then "frozen in." We may then infer from (12*b*) the relation

$$\left.\frac{du_r}{dr}\right|_{r_A} = \frac{2u_{r_A}}{r_A}u' \leq \frac{2u_{r_A}}{r_A}\left(\frac{L_P}{L_M}\right)_\infty \tag{17}$$

Since we have estimated all quantities on the right-hand side, we may put an upper limit upon the radial acceleration at r_A. Generally, L_P/L_M increases with heliocentric distance. Thus by taking the observed values for L_P/L_M at 0.3 AU, we certainly somewhat overestimate du_r/dr. For our three solar wind speed classes we quote the acceleration in Table 2, bottom panel, in the respective second columns. We infer from these parameters that the slow solar wind is smoothly accelerated at r_A, whereas the fast solar wind seems to more rapidly achieve its high speed by gaining about 50 km s^{-1} per solar radius. Thus, after about 30 R_S the high speed wind acceleration may have been completed. In contrast, low-speed wind was inferred to pass with only about 21 km/s through the Alfvén point at $r_A \approx$ 40–50 R_S. Therefore it still needs to traverse another 20 R_S in

order to finally achieve about 400 km s^{-1} in flow speed. Certainly, all these estimates are rather crude, but they open some interesting new perspectives. Helios perihelion is at about 63 R_S. Therefore Helios should be able to detect probably still ongoing acceleration in low-speed flows. Indeed, *Schwenn et al.* [1981] have reported from Helios lineup constellation that slow plasma ($v_P < 400$ km s^{-1}) beyond 0.3 AU actually further accelerates with an average increment of about (52 ± 11) km s^{-1} per astronomical unit. The flow speed in recurrent high-speed streams, though, was found to remain nearly constant which indicates that the acceleration is essentially accomplished below 63 R_S.

4. Summary and Conclusions

In this paper we have presented different but interdependent methods to deduce the values of some solar wind plasma and magnetic field parameters at the Alfvén critical point. The radial distance r_A is characterizd by the fact that the bulk flow speed reaches the local Alfvén speed and that the total specific angular momentum lost by the sun to the expanding corona and the solar wind is given by $L = \Omega r_A^2$. This latter value is the equivalent mechanical angular momentum per AMU for rigid plasma corotation. Since L involves contributions from the particles L_P and the magnetic field L_M, it does not correspond to full corotation of a plasma fluid parcel itself.

As shown in equations (10*a*), (10*b*) the slope of the radial velocity profile at r_A determines the actual fraction of plasma corotation. Smooth profiles of the logarithmic derivative $u' = d \ln u_r / d \ln r^2$ at r_A indicate a weak corotation. The case $u' = 1$ corresponds to an equipartition of stresses, where $L_M = L_P = L/2$. Steep flow velocity gradients (logarithmic) are associated with stronger corotation of the plasma, whereby magnetic field stresses play a minor role. However, for a radial flow profile with $u_r \to 0$ for $r \ll r_A$, we always find that the sun's rotation initially slows down due to magnetic stresses. Asymptotically for $r \gg r_A$, the distribution of L between L_P and L_M is solely determined by the ratio u_∞ / u_{r_A}. If the flow speed at large heliocentric distances exceeds twice the Alfvén speed at the critical point, we would expect the particles' mechanical stresses to dominate the solar wind angular momentum transport. If the wind speed at the Alfvén point reaches already more than half of the asymptotic flow speed, then most of the angular momentum loss is due to magnetic field stresses at large heliocentric distances. This situation corresponds to the original model example given by *Weber and Davis* [1967]. We should emphasize that these rather general statements can be made without solving the radial momentum equations explicitly. Clearly, for given boundary values of the plasma parameters at the sun or at the earth, say, and provided the radial evolution of the solar wind total internal energy is known, one may actually calculate the detailed radial profile of u_r. This profile then entirely determines the radial evolution of the angular momentum ratio L_P/L_M.

We have exploited the constants of motion and the theoretical expressions for L_P and L_M in section 2, in order to infer plasma parameters at the Alfvén point. For a correct evaluation of L_P it is mandatory to include the alpha particles as a major component of the solar wind plasma [*Pizzo et al.*, 1983]. Our numerical estimates are contained in Table 2. Two more or less interdependent methods have been employed. First, we directly determined r_A from L, and second, u_{r_A} from L_P/L_M and u_∞. The resulting figures are consistent with each other and show a distinct dependence on flow speed. We have already mentioned the uncertainties and problems involved in measuring u_ϕ [*Pizzo et al.*, 1983]. These need not be repeated here. However, we like to point out some other possible sources of error and limitations of our analysis:

In order to determine the true radial trends in the plasma parameters, one ideally should follow a single fluid parcel along a stream line. This can almost be achieved if data from radial lineup configurations of the Helios probes are used. Such situations, however, are rather rare. This lineup technique and our presently employed method (binning in radial distance and flow speed) yield, however, similar results, as has been shown in studies on ion adiabatic invariants by *Marsch et al.* [1983] and *Schwartz and Marsch* [1983] for our data set. Thus we can have some confidence in our results.

The real solar wind is highly structured and time dependent. Therefore, strictly speaking the homogeneous, time-stationary solar wind model of WD cannot be straightforwardly applied to real in situ observations. This may be particularly true for the angular momentum which is most sensitive to stream interactions and a possible dependence of the flow on the presently neglected azimuthal and latitudinal angular coordinates. We argue that in the body of a fast recurrent stream the in situ measurements far from the stream boundaries may yield results similar to those expected from a model high-speed stream covering 4π in spatial extent. However, this problem remains unsolved and represents the most severe limitation of our analysis. As in previous analyses we have to content ourselves with this situation, since there is no other practical way to improve the comparison of the data with theory other than by developing a full three-dimensional model for the stream-structured solar wind. However, we think that one should at least separate the data according to flow speed. This appeared to be the natural ordering scheme at least for the time around minimum solar activity.

Considering the problem with stream interactions at larger heliocentric distances, it appears imperative to use mainly data near perihelion (0.3 AU) for a reliable L or L_P/L_M evaluation. In this respect, our present data set, like the one used by *Pizzo et al.* [1983], has severe statistical limitations. On the other hand, for time periods later than mid 1976 the Helios data show a less well ordered stream structure and are possibly even more affected by small scale stream interactions. In view of our poor statistics we may really see our results as being more of qualitative nature than representing rigorous numbers. Even if we had better statistics, we could not exclude that stream interactions are possibly important all the way back from 0.3 AU into the corona and that the body of fast streams is strongly affected by surrounding flows already there. That dynamic modifications of the angular momentum transport are important at lower or even coronal levels is suggested by the predominantly negative values of L_P in fast recurrent streams. If so, we may still consider the average L as a meaningful information. However, then it is not clear why L should at all be related directly to r_A through a model-dependent relation like (3).

Many theories of coronal dynamics and solar wind expansion suggest significant acceleration of the flow beyond r_A by heat and energy or momentum disposition [*Holzer*, 1977; *Leer and Holzer*, 1980]. If these effects are important for the real solar wind, they will certainly tend to obscure or otherwise affect the value of du_r/dr as inferred by the admittedly crude method we suggest based upon relation (17).

Keeping all these limitations in mind, we may briefly summarize our main results:

The specific angular momentum of the solar wind carried by magnetic stresses is on the average $L_M = 1.07 \pm 2.25$ (AU km s^{-1}), corresponding to an equivalent azimuthal mechanical speed of about 1 km s^{-1} at 1 AU. The total flux per steradian is $\dot{M}L_M = 0.16 \pm 2.64$ ($\times 10^{30}$ dyn cm sr^{-1}). These figures are representative for all flow speeds and over the heliocentric distance range between 0.3 and 1 AU, since L_M is found to be surprisingly constant.

The particles' specific angular momentum L_P is strongly dependent on flow speed and varies with heliocentric distance. Deviations of L from the expected constancy are essentially due to variations in L_P. Whether the speed dependence of L_P is caused by interplanetary dynamics or of coronal origin must remain an open question. Probably, our data sampling technique from different stream lines may partly be responsible for this result. If this is true, the quantity L_M appears to be less sensitive to the data averaging and sampling methods used here.

Taking the data in Figure 1 and Table 1 at face value, we derived the following conclusions. The ratio L_P/L_M is strongly dependent upon the bulk flow speed. In the average solar wind we find nearly an equipartition between the particles' and fields' angular momentum. Contrarily, in slow solar wind ($v_P < 400$ km s^{-1}) most of the angular momentum lost by the sun to the solar wind is of mechanical nature with a corresponding average azimuthal flow speed up to the order of 10 km s^{-1}. This number is in accordance with earlier estimates at 1 AU [see *Lazarus and Goldstein*, 1971] that mainly stem from slow solar wind observations. Averaging over our whole data set yields $L_P/L_M = 0.8$ and $u_r = 560$ km s^{-1}.

Provided L_P is positive, the value for L_M alone places a lower limit for the location of the Alfvén radius at 11 R_S. By adding the particles' contribution L_P, one finds $r_A = 34$–49 R_S in slow, and $r_A = 14$–17 R_S in fast solar wind in agreement with earlier estimates by *Pizzo et al.* [1983].

The critical density can straightforwardly be derived from the mass loss rate $\dot{M}$ and the magnetic flux F_B, and it is about a factor of 4 larger in the slow than in the fast solar wind (see Table 2).

The Alfvén speed at r_A is only 40–50 km s^{-1} in slow speed wind, whereas we find 200–550 km s^{-1} for high-speed flows with $v_p > 600$ km s^{-1}. The direct determination of u_{r_A} is in good agreement with the one based on the continuity equation and on the estimate for r_A from L.

If we extrapolate the asymptotic values for L_P/L_M to the critical point we may even derive a crude estimate for the radial acceleration of the plasma at this point according to equation (12*b*). This concept of the ratio L_P/L_M to be "frozen in" at the critical point yields an average value of $du_r/dr \approx 51$ km s^{-1}/R_S in high-velocity streams.

In conclusion, we may say that we were able to resolve some of the discrepancies between the theory [*Weber and Davis*, 1967] and the experimental literature. Azimuthal flow speeds of a few kilometers s^{-1} are principally not in conflict with the theory. Still, it remains to be shown by detailed model calculations that a flow speed profile is possible where the asymptotic flow speed amounts to a few times its original value at r_A. In the typical high-speed solar wind the sun seems to lose its angular momentum more by magnetic than by mechanical stresses. However, values of $L_P/L_M \approx 1$ corresponding to about equipartition are also frequently observed. In low-speed wind the angular momentum appears to be mostly carried by the particles. Inferences about the critical parameters suggest a location of the Alfvén point at larger solar distances in slow solar wind than in fast streams. In addition, the plasma may partly corotate up to much larger heliocentric distances in low-speed solar wind, whereas, in fast streams it seems to be decoupled from solar rotation already at about r_A. At this point, the corresponding radial flow speed profile has been estimated to be rather steep. If the inferred gradient of 51 km s^{-1}/R_S can actually be maintained for only 10 R_S, e.g., then the typical flow speed of 680 km s^{-1} as observed at 0.3 AU might have been attained already within the first 30 R_S. Therefore high-speed flow observed by Helios at 63 R_S has essentially reached its asymptotic state. For the slow solar wind, however, it appears that there should be at least at times a fair chance to observe the wind at its stage of acceleration. Therefore the Helios probes seem to be particularly well suited to study the dynamics of the slow solar wind that at present is only poorly understood.

Acknowledgments. The authors wish to thank H. Rosenbauer, F. M. Neubauer, R. Schwenn, and W. Pilipp for making the Helios plasma and magnetic field data available for this study. The Helios plasma and magnetic field experiments and their data evaluations are supported by the German Bundesministerium für Forschung und Technologie.

The Editor thanks W. G. Pilipp and V. J. Pizzo for their assistance in evaluating this paper.

REFERENCES

Acuna, M., and Y. C. Whang, A two-region model of the solar wind including azimuthal velocity, *Astrophys. J.*, *203*, 720, 1976.

Asbridge, J. R., S. J. Bame, W. C. Feldman, and M. D. Montgomery, Helium and hydrogen velocity differences in the solar wind, *J. Geophys. Res.*, *81*, 2719, 1976.

Barnes, A., Acceleration of the solar wind by the interplanetary magnetic field, *Astrophys. J.*, *188*, 645, 1974.

Behannon, K. W., F. M. Neubauer, and H. Barnstorf, Fine-scale characteristics of interplanetary sector boundaries, *J. Geophys. Res.*, *86*, 3273, 1981.

Feldman, W. C., J. R. Asbridge, S. J. Bame, and J. T. Gosling, Plasma and magnetic fields from the sun, in *The Solar Output and its Variations*, edited by O. R. White, pp. 351–382, Colorado University Press, Boulder, Colo., 1977.

Holzer, T. E., Effects of rapidly diverging flow, heat addition, and momentum addition in the solar wind and stellar winds, *J. Geophys. Res.*, *82*, 23, 1977.

Lazarus, A. J., and B. E. Goldstein, observation of the angular-momentum flux carried by the solar wind, *Astrophys. J.*, *168*, 571, 1971.

Leer, E., and T. E. Holzer, Energy addition to the solar wind, *J. Geophys. Res.*, *85*, 4681, 1980.

Marsch, E., and A. K. Richter, Helios observational constraints in solar wind expansion, *J. Geophys. Res.*, in press, 1984.

Marsch, E., K.-H. Mühlhäuser, H. Rosenbauer, R. Schwenn, and F. M. Neubauer, Solar wind helium ions: Observations of the Helios solar probes between 0.3 and 1 AU, *J. Geophys. Res.*, *87*, 35, 1982*a*.

Marsch, E., K.-H. Mühlhäuser, R. Schwenn, H. Rosenbauer, W. Pilipp, and F. M. Neubauer, Solar wind protons: Three-dimensional velocity distributions and derived plasma parameters measured between 0.3 and 1 AU, *J. Geophys. Res.*, *87*, 52, 1982*b*.

Marsch, E., K.-H. Mühlhäuser, H. Rosenbauer, and R. Schwenn, On the equation of state of solar wind ions derived from Helios measurements, *J. Geophys. Res.*, *88*, 2982, 1983.

Meyer, F., and D. Pfirsch, Korotation und Druckanisotropien im Sonnenwind, *Kleinheub. Ber.*, *13*, 243, 1969.

Neubauer, F. M., G. Musmann, and G. Dehmel, Fast magnetic fluctuations in the solar wind: Helios 1, *J. Geophys. Res.*, *82*, 3201, 1977*a*.

Neubauer, F. M., H. J. Beinroth, H. Barnstorf, and G. Dehmel, Initial Results from the Helios 1 search-coil magnetometer experiment, *J. Geophys.*, *42*, 599, 1977*b*.

Neugebauer, M., Observations of solar wind helium, *Fundam. Cosmic Phys.*, *7*, 131, 1981.

Pilipp, W. G., R. Schwenn, E. Marsch, K.-H. Mühlhäuser, and H. Rosenbauer, Electron characteristics in the solar wind as deduced from Helios observations, Solar Wind 4, edited by H. Rosenbauer,

Rep. MPAE-W-81-31, p. 241, Max-Planck-Inst. für Aeron., Katlenburg-Lindau, Federal Republic of Germany, 1981.

Pizzo, V., R. Schwenn, E. Marsch, H. Rosenbauer, K.-H. Mühlhäuser, and F. M. Neubauer, Determination of the solar wind angular momentum flux from the Helios data—An observational test of the Weber and Davis theory, *Astrophys. J., 271*, 335, 1983.

Rosenbauer, H., R. Schwenn, E. Marsch, B. Meyer, H. Miggenrider, M. D. Montgomery, K.-H. Mühlhäuser, W. Pilipp, W. Voges, and S. M. Zink, A survey of initial results of the Helios plasma experiment, *J. Geophys., 42*, 561, 1977.

Schwartz, S. J., and E. Marsch, The radial evolution of a single solar wind plasma parcel, *J. Geophys. Res., 88*, 9919, 1983.

Schwenn, R., The "average" solar wind in the inner heliosphere: Structures and slow variations, Solar Wind 5, edited by M. Neugebauer, *NASA Conf. Publ. 2280*, p. 489, 1983.

Schwenn, R., K.-H. Mühlhäuser, E. Marsch, and H. Rosenbauer, Two states of the solar wind at the time of solar activity minimum, II, Radial gradients of plasma parameters in fast and slow streams, Solar Wind 4, edited by H. Rosenbauer, *Rep. MPAE-W-100-81-31*, p. 126, Max-Planck-Inst. für Aeron., Katlenburg-Lindau, Federal Rebpulic of Germany, 1981.

Weber, E. J., and L. Davis, The angular momentum of the solar wind, *Astrophys. J., 148*, 217, 1967.

Weber, E. J., and L. Davis, The effect of viscosity and anisotropy in the pressure on the azimuthal motion of the solar wind, *J. Geophys. Res., 75*, 2419, 1970.

E. Marsch and A. K. Richter, Max-Planck-Institut für Aeronomie, D-3411 Katlenburg-Lindau, Federal Republic of Germany.

(Received November 9, 1983;
revised March 15, 1984;
accepted March 16, 1984.)